Dependence of Width of Diverging, Plane, and Focused Transmitted Waves on Accuracy in Multipoint Simultaneous Ultrasonic Measurements of Cardiac Wall Vibration Waveform

心臓壁振動波形の超音波同時多点計測での精度の拡散波・平面波・集束波の送信幅依存性

Naoya Furusawa[1‡], Shohei Mori[2], Mototaka Arakawa[1, 2], and Hiroshi Kanai[2, 1] ([1]Grad. School Biomed. Eng., Tohoku Univ.; [2]Grad. School Eng., Tohoku Univ.)

古澤直也 [1‡]，森　翔平 [2]，荒川元孝 [1,2]，金井　浩 [2,1] ([1] 東北大院医工, [2] 東北大院工)

1. Introduction

Ultrasound diagnosis is useful for evaluating the myocardial function. However, higher spatial and temporal resolutions with high signal-to-noise ratio (SNR) are still needed for diagnosis of the heart wall which moves fast and contains inhomogeneous tissues.

In a previous study, we proposed a method of simultaneous wide-range measurement by transmitting unfocused waves such as a plane wave or a diverging wave.[1)] The method enables reduction of the number of transmissions to obtain one B-mode image and accomplishes a high frame rate measurement. However, the acoustic power of the transmisson wave decreases as the distance from the center axis of transmission waves increases, therefore, SNR decreases. Moreover, the spatial resolution in the velocity measurement is decreased by artifacts resulting from wide measurement range of the unfocused wave.

Thus, there is a trade-off relationship among the temporal resolution, the spatial resolution in the velocity measurement, and the SNR. In the present study, we examined the suitable conditions of transmission and reception considering trade-off relationship for accurate measurement of the minute vibration velocity waveform on the heart wall.

2. Methods and Experiment

The measurement of the propagation velocity of the minute vibration velocity waveform on the heart wall enables evaluation of myocardium function.[2)] As the wave length of this propagation velocity waveform is longer than 20 mm,[2,3)] it is required to measure vibrations at two points within 10 mm considering aliasing. Therefore, in the present study, two objects spaced 10 mm were used for evaluation.

The features of the diverging, plane, and focused waves are as follows. In general, the diverging wave achieves the simultaneous wide-range and high-frame-rate measurements based on the wide beam width.[1)] The focused wave achieves high spatial and contrast measurements, while its temporal resolution is degraded. The plane wave has both features of the diverging wave and the focused wave. In the present study, a collection angle θ was defined as a parameter to evaluate the features of these transmission waves. The collection angle θ is the angle between the surface of ultrasound probe and the line from the focus point to the edge of aperture (**Fig. 1**). The focal point of the diverging wave is a virtual point source O (0, r_f)} ($r_f < 0$) in Fig. 1, and that of the plane wave is at infinity ($r_f \to \infty$). Therefore, all kinds of the transmitted waves are expressed using θ: focused wave ($\theta < 90°$), plane wave ($\theta = 90°$), and diverging wave ($\theta > 90°$).

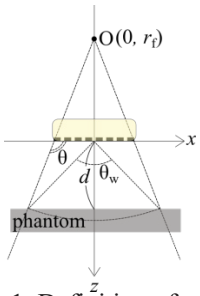

Fig. 1. Definition of collection angle θ for diverging wave.

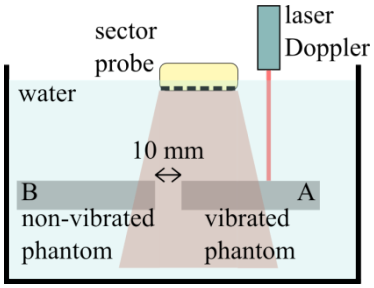

Fig. 2. Configuration of the experimental system.

In the measurement condition with the same frame rate, the focused wave has better performance, such as high spatial resolution and SNR, than the others because of narrower beam width. Therefore, the frame rates were increased as a function of the beam width to compare all kinds of transmissions at the same conditions. In the present study, the frame rate *FR* of each measurement was determined by

$$FR = f_{\mathrm{PRF}} \cdot \frac{\theta_w - \Delta\theta}{\theta_0}, \qquad \theta_w = 2\tan^{-1}\frac{d - r_f}{d\tan\theta}, \tag{1}$$

where f_{PRF} is the pulse repetition frequency, θ_w is the angular width[1)] (Fig. 1) at the range distance d, and $\Delta\theta$ is the transmitted angular interval. **Table 1** shows a list of the collection angle θ, the frame rate *FR*, and r_f which expresses the depth of the focal point (Fig. 1).

Table 1. Transmission conditions.

r_f (mm)	70	100	∞	-100	-30
θ (°)	82	84	90	96	108
FR (Hz)	279	335	558	838	1,675

Email address: n.furusawa@ecei.tohoku.ac.jp

Next, the measurement errors in the vibration velocity waveforms were evaluated as follows. A silicon rubber phantom set in the water tank was vibrated (**Fig. 2**), and its velocity was measured by ultrasound using the phased-tracking method.[3] To evaluate the accuracy of vibration velocity, the measurement error of the vibration waveform, α, was defined as

$$\alpha = \frac{\sqrt{\sum_{n=0}^{N-1}\{v_{\mathrm{L}}(n) - v_{\mathrm{U}}(n)\}^2}}{\sqrt{\sum_{n=0}^{N-1}\{v_{\mathrm{L}}(n)\}^2}}, \qquad (2)$$

where $v_{\mathrm{U}}(n)$ is the velocity measured by ultrasound, $v_{\mathrm{L}}(n)$ is the reference velocity measured by laser Doppler velocimetry (LV-1300, Ono Sokki), and N is the number of samples of the measured vibration velocity waveform.

Two phantoms A and B made in the same conditions were used in the experiment. Phantom A was set so that the edge part came the center of the ultrasound measurement area, and phantom B was located at a distance with 10 mm from phantom A. Phantom A was vibrated up and down with sine wave at 80 Hz and the maximum velocity of 40 mm/s by a shaker, while phantom B was stayed at the velocity of 0 mm/s. The depth of both phantoms was 47 mm. RF data were acquired by the ProSound-SSD α10 (Aloka) with a sector probe of 3.75 MHz of the transmitted frequency.

3. Result and Discussion

Figure 3 shows the measured minute vibration velocity waveforms. The collection angles were θ = 84°, 90°, and 108°. The amplitude of the vibration velocity measured using the diverging wave (Fig. 3(a)) was smaller than that using the others (Figs. 3(b), (c)).

The red squares (■) in **Fig. 4** show the measurement errors α under the transmitted condition listed in Table 1. At the θ = 82°, the measurement error α became large because of the aliasing of the phase difference coming from low-frame-rate acquisition. The measurement error α in the condition of the plane wave was the smallest in the transmit conditions in Table 1.

We investigated the cause of increase in measurement errors at the transmission of diverging waves. We removed the non-vibrated phantom B and measured vibration velocity of vibrated phantom A. In this case, the collection angle θ became larger, the measurement errors became smaller as shown by black circles (●) in Fig. 4.

Figure 5 exhibits the B-mode image only of non-vibrated phantom B where phantom A was removed. In Fig. 5, the artifact derived from phantom B was observed at the measurement area of vibration velocity. From these results, in the

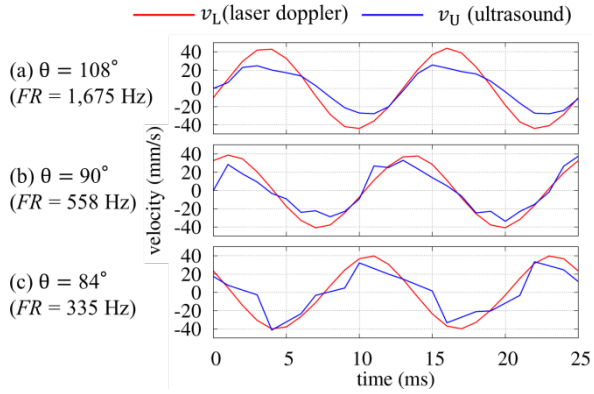

Fig. 3. The velocity waveform measured by (a) diverging wave, (b) plane wave, and (c) focused wave.

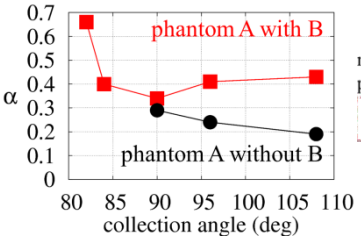

Fig. 4. Collection angle θ and the measurement error α of vibration velocity.

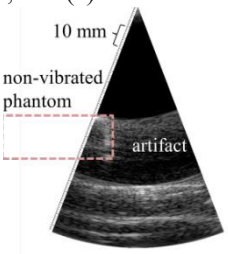

Fig. 5. B-mode image obtained with diverging wave.

experiment using two phantoms, it was suggested that the artifact from phantom B interfered in the measurement of vibration velocity of phantom A and cause large measurement errors. It is considered that the effects derived from artifact also depend on the collection angle θ and the distance from ultrasound probe to phantoms. It should be examined in detail in future work.

4. Conclusion

For determination of the suitable transmission and reception conditions of ultrasound in the measurement of the minute vibration velocity waveform on the heart wall, we evaluated the measurement accuracies of the minute vibration velocities in several conditions of transmitted waves. The relationship between the measurement accuracy and the condition of transmitted wave was quantified by considering a trade-off among the temporal resolution, the spatial resolution in velocity measurement, and the SNR. We would like to further investigate the effect of the interference of artifact from a vibrated phantom located near the observed object for accurate measurement of vibration velocity on the heart wall.

References

1. H. Hasegawa and H. Kanai: J. Med. Ultrason. **38** (2011) 129.
2. Y. Matsuno, H. Taki, H. Yamamoto, et al: Jpn. J. Appl. Phys. **56** (2017) 07JF05.
3. H. Kanai: Ultrasound Med. & Biol. **35** (2009) 936.